Indian Journal of Pure & Applied Physics
Vol. 62, October 2024, pp. 925-931
DOI: 10.56042/ijpap.v62i10.8393

Homotopy Perturbation Analysis of Steady Free Convective Flow over a Nonlinearly Stretching Sheet in an Extended Darcy-Forchheimer Porous Medium with Viscous Dissipation

A K Jhankal

Department of Mathematics, Army Cadet College, Indian Military Academy, Dehradun 248 007, India

Received 29 January 2024; accepted 20 September 2024

This study conducts an analysis to investigate the steady free convective flow over a nonlinearly stretching sheet immersed in an Extend-Darcy-Forchheimer porous medium with viscous dissipation. The governing nonlinear partial differential equations are converted into self-similar nonlinear ordinary differential equations through the application of similarity transformations. Subsequently, these transformed equations are solved using He's Homotopy Perturbation Method (HPM), a semi-exact method with the notable advantage of not necessitating a small parameter in the equations, thus circumventing the limitations associated with traditional perturbation methods. In this paper, we begin by providing a concise introduction to the fundamental principles of HPM for addressing nonlinear differential equations, followed by its application to obtain solutions for the nonlinear governing equations governing the flow, including the nonlinear term. The study also presents and discusses the effects of various relevant physical parameters on the flow.

Keywords: Free convective flow; Homotopy perturbation method (HPM); Stretching sheet; Permeability; Extend-Darcy-Forchhemer porous medium

1 Introduction

In the exploration of boundary layer flow dynamics and heat transfer characteristics surrounding a solid plate immersed in a fluid-saturated porous medium, the implications for engineering applications are profound. This analysis holds significance in diverse fields, such as enhanced petroleum resource recovery and packed bed reactor operations (Pal and Shivakumara[1]). Understanding convection through porous media extends its applicability to various domains, including geophysical flow problems, grain storage, catalytic reactors, insulation design, material conveyors, geothermal systems, and filtration devices, among others.

Numerous previous research endeavours, exemplified by Cheng and Minkowycz[2], Cheng[3], Wilks[4], Hsu and Cheng[5], Vafai and Tien[6], Soundalgekar *et al.*[7], Kaviany[8], Chen and Ho[9], Kumari *et al.*[10], Damesh and Duwairi[11], Mukhopadhyay and Layek[12], Hazarika[13], Zhang *et al*[14], Raja[15], Song *et al*,[16], Eswaramrorthi.[17], Hayat *et al.*[18], Shami *et al.*[19-20], Gul and Saeed[21], have delved into various aspects of convective flows and heat transfer. These investigations encompass topics such as free and forced convection, mixed Darcian and non-Darcian flows, variable surface temperatures, and the influence of porous media on convection.

This study introduces a novel dimension by considering the effects of Darcy-Forchheimer porous media. Darcy's law, a well-established empirical formula for forced convective flow in porous media, establishes a relationship between pressure gradient, bulk viscous fluid resistance, and gravitational force. However, deviations from Darcy's law emerge within a specific Reynolds number range (1 to 10) based on pore diameter (Ishak *et al.*[22]). For flows through porous media with high permeability, Brinkman[23] and Chen *et al.*[24] argue for the inclusion of classical frictional terms into Darcy's law. Mishra *et al.*[25] focus on Buoyancy-Driven Chemicalizer EMHD nanofluid flow through a stretching plate, while Jhankal *et al.*[26] discuss the effects of magnetic fields and thermal radiation on forced convection flow in a Darcy-Forchheimer Porous Medium.

The majority of problems in the domain of boundary layer flow exhibit nonlinear characteristics. While some problems have precise analytical solutions, many necessitate alternative methods for solving nonlinear equations. A widely accepted approach is the combination of numerical and semi-

*Corresponding author: (E-mail: anujjhankal@yahoo.com)

exact analytical methods to yield practical results. In this paper, we introduce and apply the Homotopy Perturbation Method (HPM), a semi-exact method for solving nonlinear equations, to the boundary layer flow over a stretching vertical surface with heat flux. The foundation of the HPM method was laid by He[27-31], and subsequent research by Ganji and Rajabi[32], Ganji and Sadighi[33], Ariel *et al.*[34], Zhang and He[35], Ganji and Ganjin[36], Beléndez *et al.*[37], Ma *et al.*[38], Siddiqui *et al.*[39], Zhang *et al.*[40], and Jhankal[41-42] has further advanced its application in solving nonlinear equations.

This paper specifically focuses on investigating the problem of steady free convective flow over a nonlinearly stretching sheet embedded in an Extended-Darcy-Forchheimer porous medium, considering the effects of viscous dissipation, using the Homotopy Perturbation Method (HPM). The study also delves into the influence of various physical parameters on the addressed problem.

1.1 The Fundamental concept of Homotopy Perturbation Method (HPM)

Homotopy Perturbation Method (HPM) is a mathematical technique employed to solve nonlinear differential equations within the framework of perturbation theory. This method is particularly useful when dealing with equations that involve a combination of linear and nonlinear operators, such as the one described in Eq. (1). The primary objective of HPM is to construct a solution for such equations through the introduction of an embedding parameter, p, and then obtain an approximate solution as p approaches 1.

$$A(u) - f(r) = 0, r \in \Omega \quad \dots (1)$$

Subject to the boundary conditions

$$B\left(u, \frac{\partial u}{\partial \eta}\right) = 0, r \in \Gamma \quad \dots (2)$$

Where A(u) is a differential operator, f(r) is a known analytical function, and Γ is the boundary of the domain Ω. To facilitate the solution process, the A(u) can be separated into two distinct components: L(u), which represents the linear component, and N(u), which accounts for the nonlinear component. This decomposition allows us to rewrite Eq. (1) as Eq. (3).

$$L(u) + N(u) - f(r) = 0, r \in \Omega \quad \dots (3)$$

The core concept of HPM is to introduce an embedding parameter "p" that ranges from 0 to 1. A homotopy equation "H(v,p)" is constructed (Eq. 4) as follows:

$$H(v, p) = (1 - p)[L(v) - L(u_0)] + p[A(v) - f(r)] = 0, p \in [0, 1], r \in \Omega \quad \dots (4)$$

In Eq. (4), "u_0" represents an initial approximation that satisfies the given boundary conditions. Obviously, from these definitions we will have:

$$H(v, 0) = L(v) - L(u_0) = 0$$
$$H(v, 1) = A(v) - f(r) = 0$$

The transition of the parameter "p" from 0 to 1 corresponds to the deformation of the function "v(r,p)" from its initial approximation, $u_0(r)$ to u(r). In the context of topology, this process is termed "deformation," with "$L(v) - L(u_0)$" and "$A(v) - f(r)$" referred to as homotopy functions.

HPM assumes that the solution "v(r,p)" can be expressed as a power series in "p," as indicated in Eq.(5).

$$v = v_0 + pv_1 + p^2 v_2 \quad \dots (5)$$

The solution to the original problem, u(r), is approximated as "p" tends to 1, yielding Eq. (6).

$$u = \lim_{p \to 1} v = v_0 + v_1 + v_2 + \quad \dots (6)$$

It is important to note that the convergence and stability of the HPM have been previously demonstrated in the work of Hosein Nia *et al.*[43], providing confidence in the method's applicability for solving nonlinear differential equations involving both linear and nonlinear terms.

2 Mathematical Formulation

We are concerned with the study of a steady two-dimensional laminar flow involving a viscous and incompressible fluid. This flow occurs over a continuous surface that exhibits non-linear stretching characteristics within an Extended-Darcy-Forchheimer porous medium. To describe this scenario, we employ a Cartesian coordinate system denoted by (x, y), wherein the x-axis aligns with the direction of motion along the stretching surface, and the y-axis is perpendicular to it. The surface maintains a constant temperature, denoted as Tw, while the surrounding environment possesses a temperature denoted as T∞. Notably, Tw is greater than T∞, indicating that the surface is heated (characteristic of a heated plate). The material constituting the surface is highly elastic, and it undergoes non-linear stretching at a velocity described by the function $u = u_w(x) = cx^n (n > 1)$, where c and n are constants, with n being greater than 1.

Throughout the entire flow, we make the simplifying assumption that all fluid properties

remain constant. This flow is characterized by high velocity, such that the momentum equation incorporates an additional term to account for the adjective acceleration of the fluid as well as a Forchheimer quadratic drag term. Under the standard boundary layer approximations, the governing equations for continuity, momentum, and energy, as described by Pai[44] and Schlichting[45], can be expressed as follows:

$$\frac{\partial u}{\partial x}+\frac{\partial v}{\partial y}=0 \quad \dots (7)$$

$$u\frac{\partial u}{\partial x}+v\frac{\partial u}{\partial y}=\nu\frac{\partial^2 u}{\partial y^2}-\frac{\mu}{K}u-\frac{b}{\sqrt{K}}u^2 \quad \dots (8)$$

$$\rho C_p\left(u\frac{\partial T}{\partial x}+v\frac{\partial T}{\partial y}\right)=\kappa\frac{\partial^2 T}{\partial y^2}-\frac{\partial q_r}{\partial y}+Q_0(T-T_\infty)+\mu\left(\frac{\partial u}{\partial y}\right)^2 \quad \dots (9)$$

Along with the boundary conditions are:

$$y=0: u=U_w(x)=cx^n(n>1), v=0, T=T_w$$
$$y\to\infty: u\to 0, T\to T_\infty \quad \dots (10)$$

By using the Rossel and approximation for radiation, the radiative heat flux may be simplified to be

$$q_r=-\frac{4\alpha}{3\beta}\frac{\partial T^4}{\partial y} \quad \dots (11)$$

Where α and β are the Stefan-Boltzmann constant and the mean absorption coefficient respectively. By expressing the term T^4 as a linear function of temperature using the Taylor series expansion about T_∞ and neglecting higher order terms, we get

$$q_r=-\frac{16\alpha T_\infty^3}{3\beta}\frac{\partial T}{\partial y} \quad \dots (12)$$

Using Eq. (12) energy Eq. (9) reduces to

$$\rho C_p\left(u\frac{\partial T}{\partial x}+v\frac{\partial T}{\partial y}\right)=\kappa\frac{\partial^2 T}{\partial y^2}+\frac{16\alpha T_\infty^3}{3\beta}\frac{\partial^2 T}{\partial y^2}+Q_0(T-T_\infty)+\mu\left(\frac{\partial u}{\partial y}\right)^2 \quad \dots (13)$$

The continuity Eq. (7) is satisfied by introducing a stream function Ψ such that

$$u=\frac{\partial \Psi}{\partial y} \text{ and } v=-\frac{\partial \Psi}{\partial x} \quad \dots (14)$$

The momentum and energy equations can be transformed into the corresponding ordinary nonlinear differential equations by using the following similarity transformations:

$$\eta=\left\{\frac{c(n+1)}{2\nu}\right\}^{1/2}x^{(n-1)/2}y, \Psi=\left(\frac{2\nu c}{n+1}\right)^{\frac{1}{2}}x^{\frac{n+1}{2}}f(\eta),$$
$$\theta(\eta)=\frac{T-T_\infty}{T_w-T_\infty} \quad \dots (15)$$

Where η is the independent similarity variable. The transformed nonlinear ordinary differential equations are:

$$f'''+ff''-\frac{1}{K_1}f'-(2+Fs)f'^2=0 \quad \dots (16)$$

$$\left(1+\frac{4}{3}R\right)\theta''+Pr\left(f\theta'-f'\theta+Q\theta+Ecf'^2\right)=0 \quad \dots (17)$$

The transformed boundary conditions are:

$$f(0)=0, f'(0)=1, \theta(0)=1 \text{ and}$$
$$f'(\infty)\to 0, \theta(\infty)\to 0 \quad \dots (18)$$

Where prime denotes differentiation with respect to η, $K_1=\frac{Kcx^{n-1}}{2\nu}$ is the permeability parameter, $Fs=\frac{2bx}{\sqrt{K}}$ is the Forchheimmer parameter, $R=\frac{4\alpha T_\infty^3}{3\kappa\beta}$ is the Radiation parameter, $Q=\frac{2Q_0x}{\rho C_p u}$ is the heat source parameter, $Pr=\frac{\mu c_p}{\kappa}$ is the Prandtl number and $Ec=\frac{c^2x^{2n}}{C_p(T_w-T_\infty)}$ is the Eckert number.

2.1 Solution with Homotopy Perturbation Method (HPM)

According to the HPM, the Homotopy form of Eq.(16) & (17) are constructed as follows:

$$(1-p)\left(f'''-\frac{1}{K_1}f'\right)+p\left[f'''+ff''-\frac{1}{K_1}f''-(2+Fs)f'^2\right]=0 \quad \dots (19)$$

$$(1-p)\left[\left(1+\frac{4}{3}R\right)\theta''+PrQ\theta\right]+p\left[\left(1+\frac{4}{3}R\right)\theta''+Pr\ (f\theta'-f'\theta+Q\theta+Ecf'2)=0 \quad \dots (20)\right.$$

We consider f and θ as the following:

$$u=u_0+pu_1+p^2u_2$$
$$\theta=\theta_0+p\theta_1+p^2\theta_2 \quad \dots (21)$$

By substituting Eqs (21) into (19) and (20), and then (I) Terms independent of p give

$$f_0''-\frac{1}{K_1}f_0'=0 \quad \dots (22)$$

$$\left(1+\frac{4}{3}R\right)\theta_0''+PrQ\theta_0=0 \quad \dots (23)$$

The boundary conditions are

$$f_0(0)=0, f_0'(0)=1, f_0'(\infty)=0, \theta_0(0)=1, \theta_0(\infty)=0. \quad \dots (24)$$

(II) Terms containing only p give

$$f_1'''-\frac{1}{K_1}f_1'+f_0f_0''-(2+Fs)f_0'^2=0 \quad \dots (25)$$

$$\left(1+\frac{4}{3}R\right)\theta_1''+Pr\ (Q\theta_1+f_0\theta_0'-f_0'\theta_0+Ecf_0'^2)=0 \quad \dots (26)$$

The boundary conditions are

$$f_1(0)=0, f_1'(0)=0, f_1'(\infty)=0, \theta_1(0)=0, \theta_1(\infty)=0. \quad \dots (27)$$

(III) Terms containing only p^2 give

$$f_2'''-\frac{1}{K_1}f_2'+f_0f_1''+f_1f_0''-2(2+Fs)f_0'f_1'=0 \quad \dots (28)$$

$$\left(1+\frac{4}{3}R\right)\theta_2'' + \Pr\left(Q\theta_2 + f_0\theta_1' + f_1\theta_0' - f_0'\theta_1 - f_1'\theta_0 + 2Ecf_0'f_1'\right) = 0 \quad \ldots (29)$$

The boundary conditions are

$$f_2(0) = 0, f_2'(0) = 0, f_2'(\infty) = 0, \theta_2(0) = 0, \theta_2(\infty) = 0. \quad \ldots (30)$$

(IV) Terms containing only p^3 give

$$f_3''' - \frac{1}{K_1}f_3' + f_0f_2'' + f_1f_1'' + f_2f_0'' - (2+Fs)(f_0'f_1' + f_1'^2 + f_2'f_0') = 0 \quad \ldots (31)$$

$$\left(1+\frac{4}{3}R\right)\theta_3'' + \Pr\left(Q\theta_3 + f_0\theta_2' + f_1\theta_1' + f_2\theta_0' - f_0'\theta_2 - f_1'\theta_1 + f_2'\theta_0 + 2Ecf_0'f_2' + Ecf_1'^2\right) = 0 \quad \ldots (32)$$

The boundary conditions are

$$f_3(0) = 0, f_3'(0) = 0, f_3'(\infty) = 0, \theta_3(0) = 0, \theta_3(\infty) = 0. \quad \ldots (33)$$

The Eqs (22)-(23), (25)-(26), (28)-(29) and (31)-(32) are solved with boundary conditions (24), (27), (30) and (33) respectively, the boundary condition $\eta\to\infty$ were replaced by those at $\eta=6$ in accordance with standard practice in the boundary layer analysis. If $p\to1$, we can find the approximate solution of equations (16) and (17).

3 Results and Discussion

To gain a deeper understanding of the underlying physical processes at play, we conducted numerical computations across a spectrum of physical parameters intrinsic to the governing equations. These parameters include the Permeability parameter (K_1), Stretching parameter (n), Forchheimer parameter (Fs), Radiation parameter (R), Heat source parameter (Q), Prandtl number (Pr), and Eckert number (Ec). The results of these calculations are graphically depicted in Figs 1-10, shedding light on the impacts of these parameters on velocity and temperature fields.

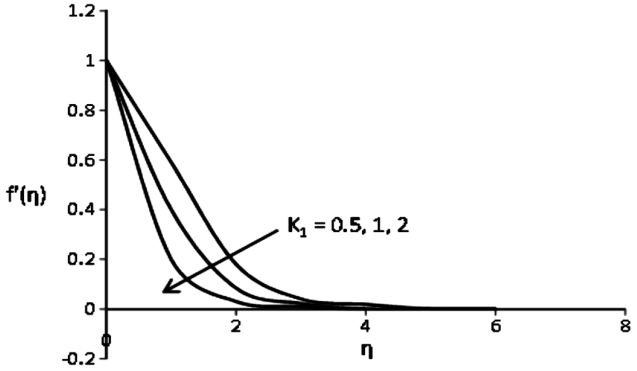

Fig. 1 — Velocity profile f'(η) for different values of K_1 when Fs=0.25 and n=1

Figure 1 portrays the influence of the Permeability parameter (K_1) on the velocity profile. It is discernible from this plot that increasing the values of the porosity parameter amplifies the velocity distribution within the flow region. Consequently, the thickness of the velocity boundary layer diminishes. This effect arises from the augmentation in horizontal velocity as the permeability of the medium increases. As permeability rises, the Darcian body force, which is inversely proportional to permeability, decreases in magnitude. This force acts to decelerate fluid particles within the medium, and as it diminishes, it results in less drag and a reduction in flow retardation. Hence, fluid velocity increases with the augmentation of K_1.

Figure 2 illustrates the temperature profiles for various values of the Permeability parameter (K_1), while maintaining constant values for n, Fs, R, Q, Pr, and Ec. Here, we observe that the temperature decreases within the boundary layer as the permeability parameter increases. This behaviour arises because the rise in permeability corresponds to a decrease in thermal diffusivity, leading to a reduction in the thickness of the thermal boundary layer.

Figures 3 & 4 depict the effects of the Stretching parameter (n) on the velocity and temperature profiles, respectively, for given values of K_1, Fs, R, Q, Pr, and Ec. Increasing values of n intensify the velocity distribution within the flow region, leading to an augmentation of the velocity boundary layer's thickness and an increase in velocity near the surface. However, a contrasting phenomenon is observed in the temperature profile for increasing values of n. This is because a higher stretching parameter minimizes thermal diffusivity, thereby decreasing the thickness of the thermal boundary layer and causing a decrease in temperature near the surface.

Figures 5 & 6 showcase the influence of the inertia parameter Fs on the velocity and temperature profiles.

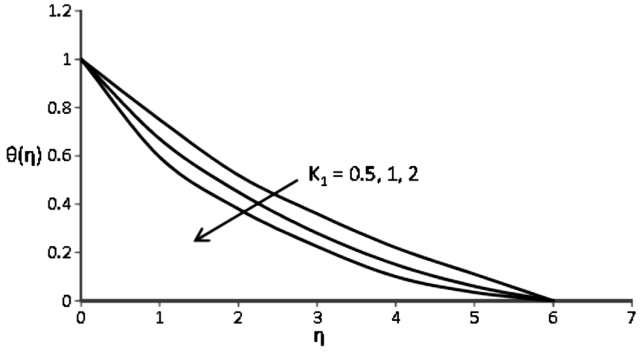

Fig. 2 — Temperature profile θ(η) for different values of K_1 when Fs=0.25, n=1, R=0.5, Q=0.2, Pr=1 and Ec=0.1

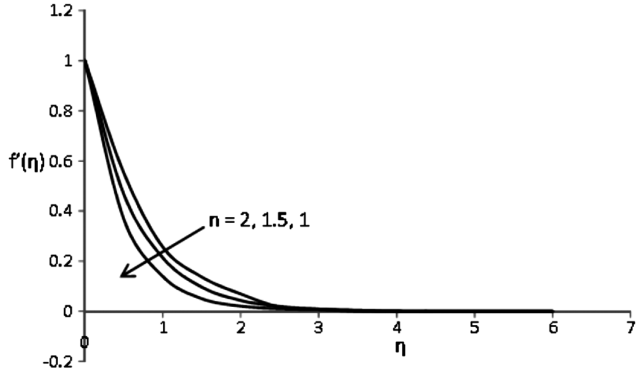

Fig. 3 — Velocity profile f'(η) for different values of n when K_1=0.5 and Fs=0.25

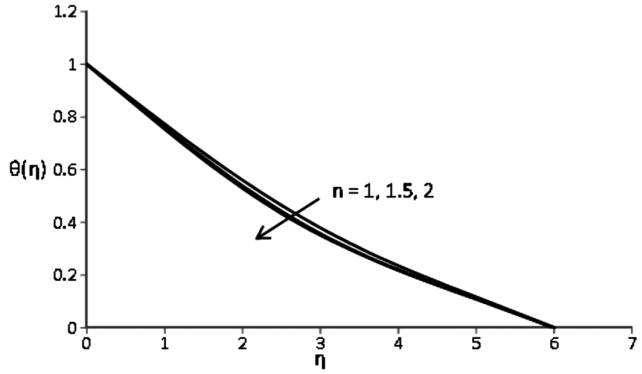

Fig. 4 — Temperature profile for different values of n when K_1=0.5, Fs=0.25, R=0.5, Q=0.2, Pr=1 and Ec=0.1

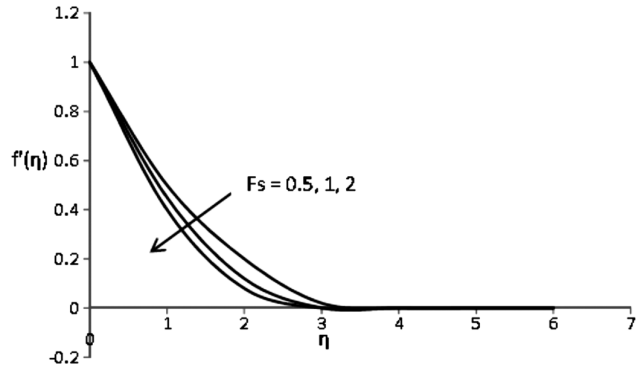

Fig. 5 — Velocity profile for different values of Fs when K_1=0.5 and n=1

It is evident from these figures that an increase in the value of Fs results in a decrease in the velocity profile, particularly at the surface. This phenomenon occurs due to an increase in the form drag of the porous medium when the inertia effect is considered. In contrast, the temperature profile increases with an increase in the inertia parameter Fs.

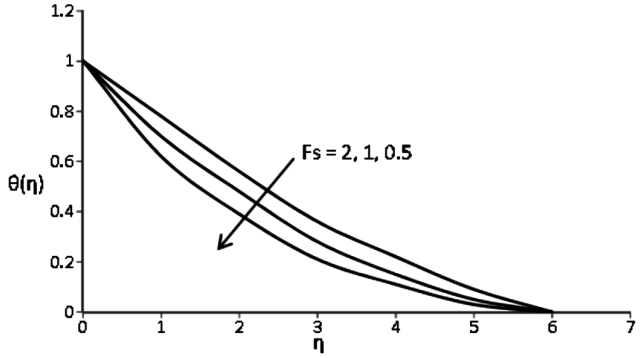

Fig. 6 — Temperature profile for different values of Fs when K_1=0.5, n=1, R=0.5, Q=0.2, Pr=1 and Ec=0.1

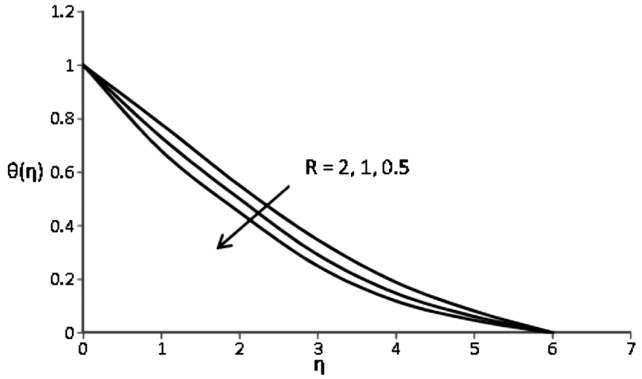

Fig. 7 — Temperature profile for different values of R when K_1=0.5, n=1, Fs=0.25, Q=0.2, Pr=1 and Ec=0.1

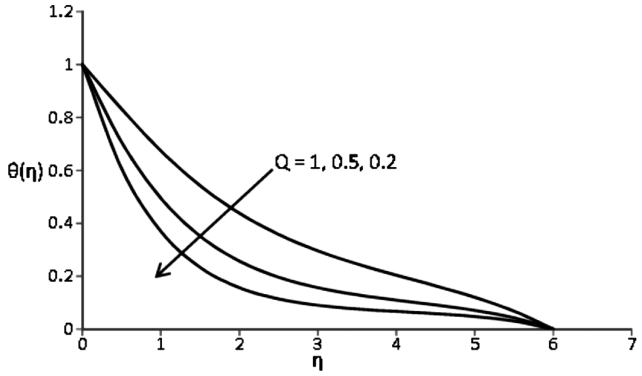

Fig. 8 — Temperature profile for different values of Q when K_1=0.5, n=1, Fs=0.25, R=0.5, Pr=1 and Ec=0.1

Figure 7 demonstrates the effect of the Radiation parameter (R) on the temperature profile. From this figure, we infer that an increase in R leads to an increase in temperature. This is attributed to the amplified radiation within the thermal boundary layer, resulting in higher temperature profiles.

Fig. 8 reveals the impact of the Heat source parameter (Q) on the temperature profiles. It is

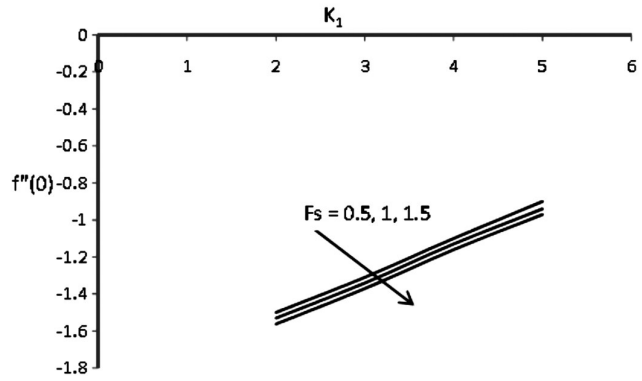

Fig. 9 — Variation of $f''(0)$ with K_1 for different values of Fs when n=1

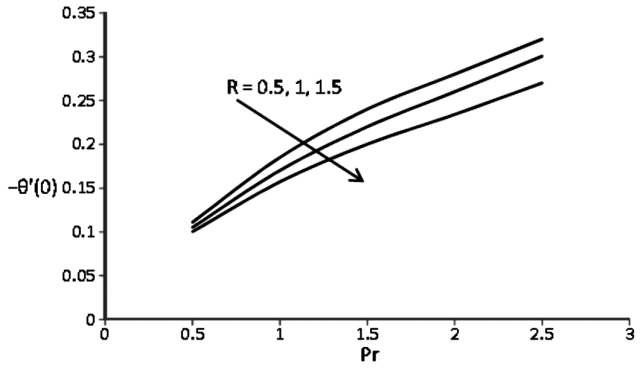

Fig. 10 — Variation of –θ'(0) with Pr for different values of R when K_1=0.5, n=1, Fs=0.25, Q=0.2 and Ec=0.1

evident that temperature increases as Q is raised, indicating that heat source parameter manipulation can be employed to control the temperature fields.

Skin friction, computed against K_1 for various values of Fs, is illustrated in Fig. 9. It is clear from this graph that skin friction decreases with an increase in Fs but increases as K_1 increases.

Finally, Fig. 10 presents the rate of heat transfer, as measured by the Nusselt number. Increasing the Prandtl number (Pr) enhances the heat transfer coefficient, with positive Nusselt numbers indicating heat transfer from the surface to the medium. Additionally, an increase in R leads to a decrease in the Nusselt number.

4 Conclusion

In conclusion, this study has introduced a mathematical model to describe two-dimensional steady free convective flow over a nonlinearly stretching sheet immersed in an Extend-Darcy-Forchheimer porous medium with viscous dissipation. By applying similarity transformations, the governing partial differential equations were transformed into ordinary differential equations. These nonlinear ordinary differential equations were then successfully solved using the Homotopy Perturbation Method. The investigation of physical parameters controlling velocity and temperature profiles, as presented graphically, revealed several key findings:

(a) The velocity increases with higher values of the permeability parameter and stretching parameter, but it decreases as the Forchheimer parameter increases.
(b) Temperature decreases with increasing values of the permeability parameter and stretching parameter, while it increases with a higher Forchheimer parameter.
(c) Temperature increases with rising radiation parameter and heat source parameter values, resulting in an increased thickness of the thermal boundary layer.
(d) Skin friction coefficient decreases as the Forchheimer parameter increases but increases with higher permeability parameter values.
(e) Nusselt number increases with an increase in Prandtl number but decreases with higher radiation parameter values.

It is worth noting that the Homotopy Perturbation Method (HPM) employed in this study has proven to be an effective approach for solving nonlinear differential equations. Thus, this method stands as a valuable mathematical tool with the capability to address both linear and nonlinear systems of differential equations. The results obtained from this study can serve as a foundation for understanding and predicting complex fluid dynamics in porous media, contributing to various practical applications in engineering and physics.

Nomenclature

b Local inertia coefficient
c Constant
C_p Specific heat at constant pressure
f Dimensionless stream function
Ec Eckert number
Fs Forchheimmer parameter
K Darcy permeability of the porous medium
K_1 Permeability parameter
n Stretching parameter
Pr Prandtl number
q_r Radioactive heat flux
Q_0 Rate of heat generation

Q Heat source parameter
R Radiation parameter
T Temperature of the fluid
u, v Velocity component of the fluid along the x and y directions, respectively
x, y Cartesian coordinates along the surface and normal to it, respectively

Greek symbols

α Stefan-Boltzmann constant
β Mean absorption coefficient
Ψ Stream function
η Similarity variable
ρ Density of the fluid
μ Viscosity of the fluid
κ Thermal conductivity
υ Kinematic viscosity
θ Dimensionless temperature

Superscript

‘Derivative with respect to η

Subscripts

w Properties at the plate
∞ Free stream condition

References

1 Pal D & Shivakumara I S, *Int J Appl Mech Eng*, 11(4) (2006) 929.
2 Cheng P & Minkowycz W J, *J Geophys Res*, 82 (1977) 2040.
3 Cheng P, *Int J Heat Mass Transf*, 20 (1977) 201.
4 Wilks G, *Int J Heat Mass Transf*, (1973) 16.
5 Hsu C T & Cheng P, *Int J Heat Mass Transf*, 28 (1985) 683.
6 Vafai K & Tien C L, *Int J Heat Mass Transf*, 24 (1981) 195.
7 Soundalgekar V M, Takhar H S & Vighnesam N V, *Nucl Eng Des*, 110 (1988) 95.
8 Kaviany M, *ASME J Heat Transf*, 109 (1987) 345.
9 Chen K S & Ho J R, *Int J Heat Mass Transf*, 29 (1988)753.
10 Kumari M, Pop I & Nath G, *Acta Mech*, 84 (1990) 201.
11 Duwairi H M & Damseh R, *Can J Phys*, 87 (2009) 161.
12 Mukhopadhyay S & Layek G C, *Meccanica*, 44 (2009) 587.
13 Hazarika G C, World Academy of Science, *Engineering and Technology*, (2013) 77.
14 Zhang L, Bhatti M M & Michaelides E E, *Int J Numer Methods Heat Fluid Flow,* 31 (2020) 2623.
15 Raja M A Z, Khan Z, Zuhra S, Chaudhary N I, Khan W U, He Y, Islam S & Shoaib, M, *Case Stud Therm Eng,* 26 (2021) 101168.
16 Song Y Q, Khan S A, Imran M, Waqas H, Khan S U & Khan M I, *Alexandria Eng,* 60 (2021) 4607.
17 Eswaramoorthi S, Loganathan K, Faisal M, Botmart T & Shah N A, *Ain Shams Eng J*, 14 (2022) 101887.
18 Hayat T, Haider F, Muhammad T & Alsaedi A, *J Mol Liq*, 233 (2017) 278.
19 Shami S, Sajid M & Javed T, *Waves in Random & Complex Media,* 10 (2023) 2177497.
20 Shami S, Sajid M & Javed T, *Proc of the Instititution of Mech Eng Part E: J of Process Mech Eng,* 1177 (2022).
21 Gul T & Saeed A, *Waves in Random and Complex Media*, (2022) 2077471.
22 Ishak A, Nazar R & Pop I, *Int J Appl Mech Eng*, 11(3) (2006) 623.
23 Brinkman H C, *Appl Sci Res*, 1 (1947) 27.
24 Chen C K, Chen C H, Minkowycz W J & Gill U S, *Int J Heat Mass Transfer*, 35 (1992) 3041.
25 Mishra S R, Shahid A, Jena S & Bhatti M M, *Heat Transfer Res*, 50(11) (2019) 1105.
26 Jhankal A K, Jat R N & Kumar Deepak, *Int J Curr Res Rev*, 9(11) (2017) 16.
27 He J H, *J Comput Math Appl Mech Eng*, 167 (1998) 57.
28 He J H, *Int J Non-linear Sci Numer Simul*, 1 (2000) 51.
29 He J H, *Int J Nonlinear Sci Numer Simul*, 2 (2001) 317.
30 He J H, *Int J Non-linear Sci Numer Simul*, 6 (2005) 207.
31 He J H, *Comp Math Appl*, 57(3) (2009) 410.
32 Ganji D D & Rajabi A, *Int Comm Heat Mass Transfer*, 33 (2006) 391.
33 Ganji D D & Sadighi A, *Int J Nonl Sci Num Simul*, 7(4) (2006) 411.
34 Ariel P D, Hayat T & Asghar S, *Int J Nonlinear Sci Numer Simul*, 7(4) (2006) 399.
35 Zhang L N & He J H, *Mathematical Problems in Engineering*, 83878 (2006).
36 Ganji Z Z & Ganji D D, *Int J Nonlinear Sci Numerical Simul*, 9(4) (2008) 415.
37 Beléndez A, Beléndez T, Márquez A & Neipp C, *Chaos Solitons Fractals*, 37(3) (2008) 770.
38 Ma X, Wei L & Guo Z, *J Sound Vibrat*, 314 (2008) 217.
39 Siddiqui A M, Zeb A, Ghori Q K & Benharbit A M, *Chaos, Solitons Fractals*, 36(1) (2008) 182.
40 Zhang B G, Li S Y & Liu Z R, *Phys Lett A*, 372(11) (2008) 1867.
41 Jhankal A K, *J Appl Fluid Mech*, 7(1) (2014) 177.
42 Jhankal A K, *Chem Eng Res Bullet*, 18 (2015) 12.
43 Hosein Nia S H, Ranjbar A N, Ganji, D D, Soltani H & Ghasemi J, *Phys Lett A*, 372(16) (2008) 2855.
44 Pai S I, *Viscous Flow Theory: I – Laminar Flow,* (DVanNostrand Co: New York), 1956.
45 Schlichting H, *Boundary layer theory", 6th edn*, (McGraw-Hill: New York), 1968.